5 Weld strength estimation using a data-driven approach

In the previous section, a real-time monitoring approach based on the changes in the amplitude of the horn and anvil vibrations was presented. In doing so, the horn and anvil measurements were divided into welding stages corresponding to the development of the weld. The goal of this section is to build on this knowledge to find features which may be used to monitor the welding process in real time. To do so, features which can be directly related to the progress of the welding process are used. These features can be used to either track the welding process through its stages, identify when a weld enters its stage 5 and reaches its maximum strength, or to estimate the strength of different welds within the same stage. In addition, the reliability of these features in tracking the welding stages is investigated.

5.1 Features for welding stage monitoring[2]

5.1.1 Motivation and approach

The goal of this section is to present features which can help track the transition from one welding stage to another. Based on the information in Chapter 4.2, USMW can be optimized by tracking the welding stages and ensuring that the welding process is stopped in a weld's stage 5, where its strength reaches its maximum. These features can be used to identify the start of stage 5, and stop the welding process then. It can also be useful for other research to know when any of the other welding stages start and end. In tracking the welding stages during welding, researchers can relate their research to the thermo-mechanical processes taking place during welding by just tracking the vibrations of the horn or anvil.

To do so, and since the monitoring approach described in Chapter 1 relies on detecting changes in the amplitude of the envelopes of the horn and anvil, their rates of change with welding time are studied. This approach is constrained to the vibrations at the welding frequency, which were the only ones to show changes in behavior at the transition of all welding stages. From these vibrations features are extracted and used to separate the weld groups. The curves of the

[2] Part of this subchapter were published in [33]

rate of change are also divided into the welding stages and their behavior described.

5.1.2 Data processing

The data used in this section is the envelopes of the horn and anvil vibrations as described and processed in Chapter 4.

To extract the trends in the envelopes while minimizing the influence of high-frequency noise, the rate of change in the envelope amplitudes over a period of 0.02 s was calculated. This was done using 0.02 s sliding windows with 50% overlap. This was done using a forward differentiation method, in which the sum of the amplitudes of the envelope at the end and the beginning of each window was divided by the length of the window. Here as well, the length of 0.02 s was chosen after some experimentation with different window sizes, and smaller windows were still too sensitive to short term noise. The calculation process is stopped when the sliding window reaches the end of welding, such that the strong decrease in amplitude at the end of welding is not included in the rate of change, as shown in Figure 5-1. The process is described as follows:

Equation 1

$$R_{t=0.02*\frac{n+1}{2}} = \frac{En_{t=0.02*\left(\frac{n}{2}+1\right)} + En_{t=0.02*\left(\frac{n}{2}\right)}}{0.02}$$

where R is the rate of change, En is the amplitude of the envelope, t is the time, and $n = [1,2,3 \dots]$ is the number of the sliding window.

After extracting the rate of change, it was further smoothed using a 0.01 s moving average.

It should be noted that small differences in the stage start and end times between Chapter 4.2 and the analysis below are due to the processing to extract the rate of change and to individual differences between welds, which did not influence the results in Chapter 4.2.

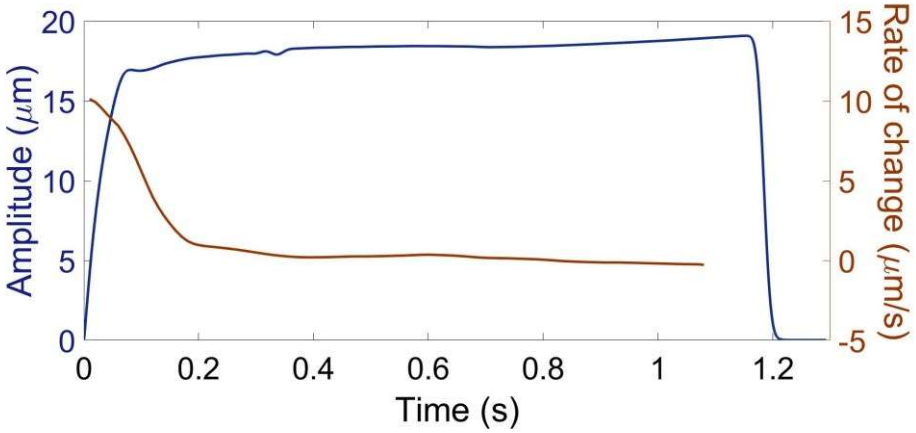
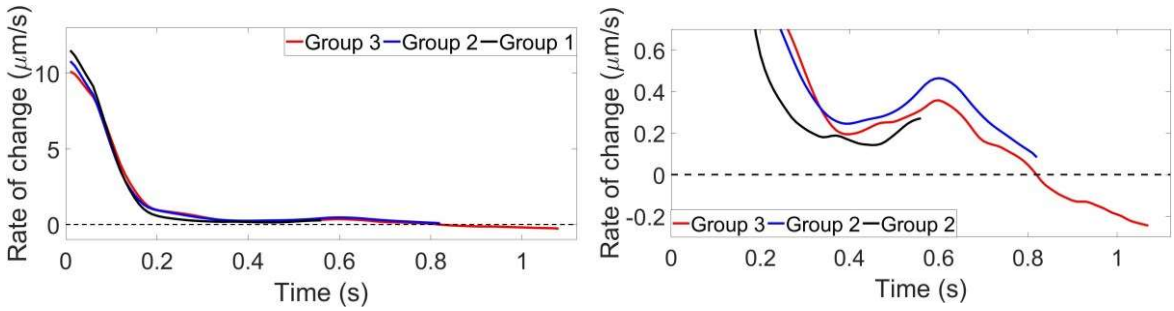


Figure 5-1: An envelope of horn vibrations and its rate of change

5.1.3 Features from the anvil vibrations



(a) (b)

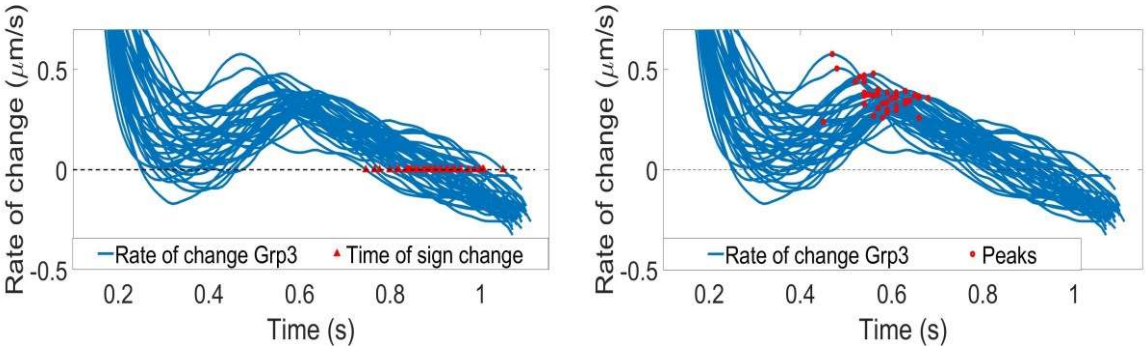
Figure 5-2: Rate of change of the anvil envelopes for groups 1, 2 and 3, with (a) a full view and (b) a zoomed view. Group 1 in black, Group 2 in blue, Group 3 in red.

Figure 5-2(a) and (b) show plots of the rate of change of a single anvil envelope from each of groups 1, 2 and 3, and which are representative of their groups. Similar to the signals in Figure 4-8, the curves of the three groups overlap well. It is therefore sufficient to discuss group 3 to represent the entire welding process.

From Figure 5-2(a), it can be seen that the rate of change starts positive and decreases rapidly from the beginning of welding until about 0.2 s: this denotes stage 1, in which the anvil starts getting excited. As the envelope amplitude gets closer to its steady-state vibrations, the rate of change decreases. The rate of change decreases more slowly from 0.2 s until about 0.35 s or 0.4 s: this corresponds to stage 2, where the cleaning and shearing process means that some of the kinetic energy from the horn gets transferred into the shearing process, leading to less excitation of the anvil, which then increases in amplitude at a slower

rate. Stage 3 starting around 0.35 s or 0.4 s. From Figure 5-2(b), the rate of change increases until a peak is reached around 0.6 s: this means that the envelope is increasing at an increasing rate. The peak denotes the start of stage 4. Starting 0.6 s, the rate of change decreases, though is still positive. This decrease can be explained by the increasing relative movement at the horn-workpiece and workpiece-anvil interfaces, which mean a decreasing excitation of the anvil as less energy is transferred to it. Around 0.8 s, the rate of change crosses zero and becomes negative, showing that the amplitude of the envelope started decreasing, and indicating the start of stage 5. At that point, relative movement at the horn-workpiece and workpiece-anvil interfaces has increased to the point that the anvil is not excited enough to maintain its amplitude of vibration, which then decreases. The timing of these stages corresponds with those from Chapter 4.2.

Figure 5-3(a) shows the rate of change of all 40 welds of group 3, as well as the moment each of the crosses the 0 line, which ranges from 0.75 s to 1.1s. From the figure, it is clear that the moment of zero crossing is different for each line, meaning that each weld enters stage 5 at a different moment. This was not apparent from looking at the envelopes in Figure 4-8. From this information, it is possible to clearly identify the start of stage 5 by detecting the moment the rate of change of the anvil amplitude becomes negative. Figure 5-3(a) also shows that some curves cross the zero line earlier than stage 5, between 0.2 s and 0.4 s, so merely detecting a change of sign is not enough.



(a) (b)

Figure 5-3: Rate of change of all group 3 welds. (a) shows the points where the rate of change crosses zero, showing the start of stage 5, and (b) shows the peaks of the curves, which denote the start of stage 4.

From Figure 5-3(a), it can be seen that all curves show a peak at the beginning of stage 4. The peaks are clearly shown in Figure 5-3(b), and fall between 0.5 s

and 0.7 s. Practically, this means that it is possible to detect the start of stage 5 in the rate of change of the anvil envelope by first detecting the peak of stage 4, and then detecting the change of sign after the peak.
Table 5-1 shows the number of welds for which the rate of change showed a peak between 0.4 s and 0.7 s followed by a change of sign from positive to negative. All group 2 and group 3 welds showed a peak, meaning they entered stage 4. This was expected based on the results in Chapter 4. However, two group 1 welds also showed a peak, which would indicate they had just entered stage 4. As for the change of sign after the peak, all group 3 welds and no group 1 weld showed a change of sign, which was expected. As for group 2 welds, three welds from group 2 showed a change of sign, indicating they probably started their stage 5, while the others were close to changing signs. A monitoring algorithm based on detecting the sign of the rate of change would have classified these group 2 welds as group 3. However, this is not a problem, since there is no difference in strength between group 2 and group 3, as mentioned in 4.
Based on the information in this section, it is possible to monitor USMW by detecting when a weld enters its stage 5 using the rate of change of the anvil envelope.

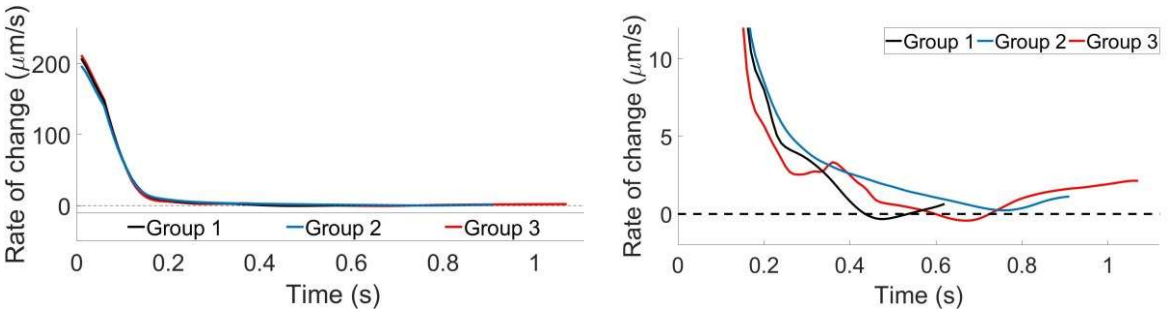
Table 5-1: Number of welds in which the rate of change of the anvil envelope had a peak between 0.4 s and 0.7 s and a change of sign following it

Ratio (and %) of welds which showed…	Group 1	Group 2	Group 3
peaks between 0.4 s and 0.7 s	2/40 (5%)	40/40 (100%)	40/40 (100%)
a change of sign following the peak	0/40 (0%)	3/40 (7.5%)	40/40 (100%)

5.1.4 Features from the horn vibrations

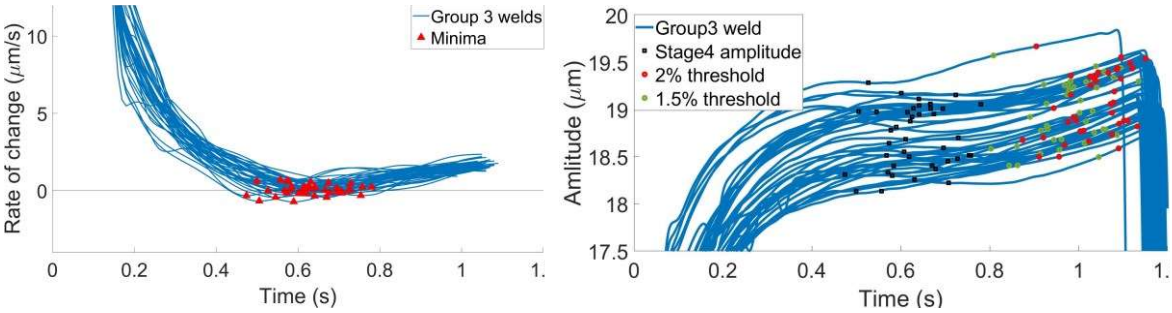
Figure 5-4 shows the rate of change of one horn envelope from each of groups 1, 2 and 3. The common features for all curves were a start from a high positive value in the beginning of welding until 0.2 s, which indicates the first stage of welding. This was followed by a slower decrease until a minimum is reached between 0.4 s and 0.8 s, after which the rate of change increases again. When approaching its minimum, some rates of change become negative, as the group 1 and group 2 welds in Figure 5-4(b) do. The minima for all group 3 welds are

shown in Figure 5-5(a). Comparing these minima to the results from Chapter 5.1.3, they roughly fall within the same time frame as the peaks of the anvil curves shown in Figure 5-3(a), showing that these minima could indicate the start of stage 4. Contrary to the anvil plots, the horn plots do not show any distinctive feature which could indicate the start of stage 3 or the start of stage 5.



(a) (b)

Figure 5-4: Rate of change of the horn envelopes for groups 1, 2 and 3, with (a) a full view and (b) a zoomed view. Groups 1, 2 and 3 in black, blue and red.



(a) (b)

Figure 5-5: (a) Rate of change of the horn envelopes and the minima of all welds. (b) Horn envelope, stage 4 amplitudes, and stage 5 threshold values for both 1.5% and 2% changes.

Nevertheless, it is possible to estimate when a weld is in stage 5 by using the rate of change in conjunction with the horn envelope. According to Figure 5-5(a), since the rate of change is positive after the minima, the amplitude of the horn vibrations increases during stage 4 and 5. This is in line with the expectations from [1]. In this case, it would be possible to identify a stage 5 weld by the increase of the amplitude of its horn vibrations relative to its stage 4 amplitude: when the horn amplitude increases by a certain amount compared to its stage 4 amplitude, then the weld is in stage 5. The value of the stage 4 amplitude can be taken as the horn amplitude when its rate of change reaches a minimum.

With this approach, the start of stage 5 cannot be detected, but the presence of a weld in stage 5 could be estimated.
The next step is to set the threshold value. In this study, two thresholds were tested: a 1.5% increases compared to the stage 3 or 4 amplitude, and a 2% increase. This was tested on all welds of all groups. The results are shown in Table 5-2, and the stage 4 and stage 5 threshold amplitudes for both 1.5% and 2% are shown in Figure 5-5(b) for group 3. From Figure 5-5(b), it can be seen that with a 1.5% threshold, a stage 5 was detected as early as 0.8 s, while with a 2% threshold, a stage 5 was detected starting 0.88 s. Both of these time points occur later than the change of sign of the anvil slopes in Figure 5-2(b). In this way, the threshold could be set depending on how early the user would like to detect that a weld is in stage 5. From the performance in Table 5-2, the 1.5% threshold could identify all group 3 welds and even two of the group 2 welds, while falsely identifying one group 1 weld as being in stage 5. Upon closer inspection, this false positive was due to a misdetection of the minimum of the rate of change. With a 2% threshold, there were no false positives. However, one stage 3 weld could not be detected because the threshold value was not reached.

Table 5-2: Number of welds which reached the horn stage-5-threshold value

	Group 1		Group 2		Group 3	
1.5% threshold	1/40	2.5%	2/40	5%	40/40	100%
2% threshold	0/40	0%	1/40	2.5%	39/40	97.5%

In this way, it is possible to use the horn vibrations to detect when a weld is in stage 5. However, the process relies on establishing a suitable threshold, and is more prone to errors than using the anvil vibrations.

5.1.5 Real-time usability of the approach

To estimate whether the use of the rate of change and its characteristic points can be used for a real-time monitoring of the welding process, the time required to calculate the rate of change from the smoothed envelopes of Chapter 4 and the time required to identify the start of stage 5 is calculated. This is done using a smoothed envelope of the anvil vibrations, since the anvil was found to be more robust in identifying the start of stage 5. The process was repeated 1000 times and the mean and standard deviation are returned.

Calculating the rate of change in the code used for this thesis took on average 29.7 ms with a standard deviation of 2.8 ms, and the identification of the start of stage 4 and the start of stage 5 took on average 0.024 ms with a standard deviation of 0.12 ms. Most of the processing time was therefore used to calculate the rate of change. Adding the 29.7 ms for the rate of change to the 35.7 ms needed to create the smoothed envelopes from the raw data would place the processing time at 65.4 ms, which is still well in the order of magnitude of real-time processing. The approach would therefore not be usable for real-time processing according to the requirements set in Chapter 0.
However, the processing time still falls within the 0.1 s welding stage duration set in Chapter 0, which is expected to be shorter than many welding application. For example, in this study, the length of stage 5 is about 0.2 s long. Furthermore, the current implementation of the code includes operations which would not be needed in a practical implementation, for example the use of the "*find*" function twice to extract the amplitude of the smoothed envelope at the correct times, and an implementation of the approach optimized for speed in an appropriate low-level language should achieve shorter computation times. It is therefore possible to use the approach for real-time monitoring.

5.1.6 Conclusion on features for welding stage monitoring

The analysis of the rate of change of the horn and anvil vibrations showed that all stages could be clearly detected in the anvil vibrations using either inflection points or zero crossings, while only stages 4 could be detected as clearly in the horn vibrations. Furthermore, the anvil vibrations are more reliable in detecting the start of stage 5 than the horn vibrations. For these reasons, using the anvil vibrations seems preferable to monitor the progress of the welding process through its welding stages than the horn vibrations. With regards to real-time implementations of this approach, the total time required to produce the smoothed envelope of the raw measurement data, calculate its rate of change and identify the start of stage 5 was found to be 65.4 ms. This duration is short enough to monitor the welding process in this study but does not meet the 50 ms requirement previously set in Chapter 0 which is expected to make the approach suitable for much shorter welding processes. However, since the 50 ms is only exceeded by a short time and the code can be implemented more efficiently, then the monitoring approach is still suitable for real-time monitoring of USMW.

5.2 Features for weld strength estimation

5.2.1 Motivation and approach

In Chapter 5.1, features to monitor the strength of welds by monitoring welding stages were presented. In this section, features to estimate the weld strength for welds within the same welding stage are presented. This is done on the group 3 welds, as they include the longest welding time while having strong welds. To do so, many features are extracted from the envelopes of the horn and anvil vibrations. All features studied have a clear relation to the welding process and the different welding stages. For the weld strength estimation, the real-time monitoring potential is not investigated because it is highly dependent on the choice of algorithm, which is not investigated in this thesis.

5.2.2 Features extraction

The features are extracted from the horn and anvil envelopes produced in Chapter 4. They are therefore dependent on the data processing used in Chapter 5.1. The features can be divided into three categories: time-related features, amplitude-related features, and time-and-amplitude-related features. Some of the features are shown in Figure 5-6.

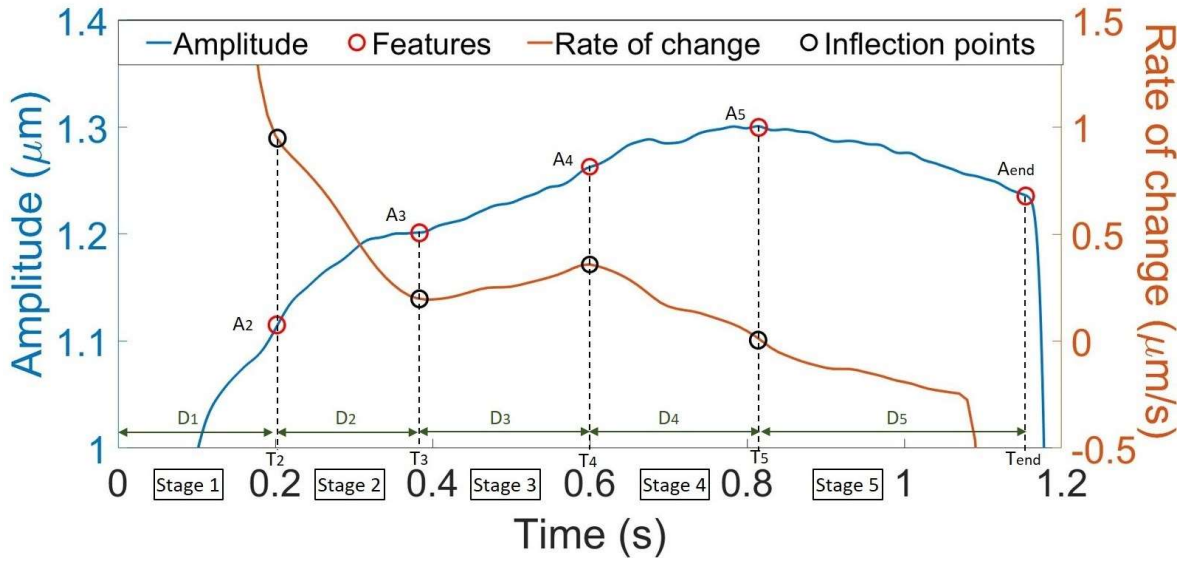


Figure 5-6: Features extracted from the anvil envelope, rate of change and second order rate of change

5.2.2.1 *Time-related features*

The amount of time a weld spends in a welding stage might relate to the weld strength. For example, it is possible that welds spending more time in stage 4, the strengthening stage, are stronger than welds spending less time in it, or that welds spending longer in stage 2, a stage in which the weld is neither formed nor strengthened, consume too much energy for this stage and have too little energy left for the other stages. For this reason, time-related features such as the duration of a welding stage or the start time of a welding stage are investigated. One set of features is the start of each welding stage and the end of welding. For each measurement, the start time of each welding stage is detected using the rate of change of the anvil envelope extracted in Chapter 5.1 and presented in Figure 5-3. The start of stages 3, 4 and 5 are detected by the minimum, maximum and the change of sign described in Chapter 4.2.2. To detect the start of stage 2, since the rate of change and its derivative did not show a clear start, the second derivative of the rate of change, not shown here, was used. In stage 1, this second derivative is negative with a positive slope, since the rate of change decreases with decreasing slope, and then reaches a constant value when the rate of change reaches its slower decrease described in Chapter 4.2.2. The start of stage 2 was taken as the first value of the second derivative larger than -10^{-5} $m.s^{-2}$. The time for the end of welding was calculated by taking the derivative of the horn amplitudes and detecting when the amplitude started to rapidly decrease, indicating the end of welding. These features are shown in Table 5-3.

Table 5-3: Features related to the start times of the welding stages and the end of welding

	Start of stage 2	Start of stage 3	Start of stage 4	Start of stage 5	End of welding
Feature	T_2	T_3	T_4	T_5	T_{END}

The next set of features is the duration of the welding stages, calculated using the previous features. The duration of each stage is interesting to look at because it gives an idea of how long a specific thermo-mechanical process occurred. Welds with a longer stage 2 might be “cleaner” than welds with shorter stages 2 leading to a better weld creation, or the longer stage 2 would indicate that more of the total energy input by the welding machine to the workpieces went

to the stage, leaving less energy for the other stages with a more direct impact on the weld strength. Welds with a longer stage 3 would have spent more time in the weld creation stage, which might indicate a larger or denser weld area. Welds with a longer stage 4 would have spent more time in the strengthening stage, leading to a stronger weld. Welds with longer stage 5 could be closer to overwelding, and might therefore be weaker. These features and the equations to calculate them are shown in Table 5-4.

Table 5-4: Features related to the duration of each welding stage

Feature	Equation	Relation to the welding process
D_1	$T_2 - 0$ s	Duration of stage 1
D	$T_3 - T_2$	Duration of stage 2
D_3	$T_4 - T_3$	Duration of stage 3
D_4	$T_5 - T_4$	Duration of stage 4
D_5	$T_{end} - T_5$	Duration of stage 5

From the welding stage durations calculated, some meta-durations are defined. These durations give an indication of larger mechanical processes, such as the duration in which the weld goes through mechanical transformations before reaching its maximum strength, which corresponds to stages 3 and 4. These features are listed in Table 5-5.

Table 5-5: Features created by summing durations of welding stages

Feature	Equation	Relation to the weld strength.
L_{34}	$= \sum_{i=3}^{4} D_i$	Length of time of weld formation (stage 3) and strengthening (stage 4)
L_{345}	$= \sum_{i=3}^{5} D_i$	Length of time of weld formation (stage 3), strengthening (stage 4), and time in the optimal stage (stage 5)
L_{45}	$= \sum_{i=4}^{5} D_i$	Length of time of weld strengthening through strengthening (stage 4) and time in the optimal stage (stage 5)

Furthermore, to investigate whether the relation between the lengths of different stages impact the weld strength, for example the strength of a weld which has spent less time forming a weld and more time strengthening the weld, ratios of the durations are calculated. These are shown in Table 5-6.

Table 5-6: Ratios of durations of different stages of welding

Fea-ture	Equa-tion	Relation to the weld strength
DL_{3345}	$= \frac{D_3}{L_{345}}$	The duration of the weld formation stage compared to the length of time of weld formation, strengthening, and time in the optimal stage
DL_{4345}	$= \frac{D_4}{L_{345}}$	The duration of the weld strengthening stage compared to the length of time of weld formation, strengthening, and time in the optimal stage
DL_{5345}	$= \frac{D_5}{L_{345}}$	The duration of the weld strengthening stage compared to the duration of weld formation and strengthening
DD_{33}	$= \frac{D_3}{D_4}$	The duration of the weld formation stage compared to the length of time of weld formation, strengthening, and time in the optimal stage
DD_{35}	$= \frac{D_3}{D_5}$	The duration of the weld formation stage compared to the length of time of weld formation, strengthening, and time in the optimal stage
DD_{45}	$= \frac{D_4}{D_5}$	The duration of the strengthening stage compared to the length of time of weld formation, strengthening, and time in the optimal stage

5.2.2.2 *Amplitude-related features*

The amplitudes of the horn or anvil vibrations at the points measured in this thesis are related to the amount of slip between the horn and the anvil: a strengthening of the connection between them leads to an increase in the anvil vibrations and a decrease in the horn vibrations due to more excitation of the anvil and more loading on the horn respectively.

For this reason, the amplitude of the horn and anvil vibrations at the end of each welding stage are used as features. The amplitudes extracted are the amplitudes of the smoothed envelopes the anvil and horn vibrations at the start of each

welding stage and the end of welding. Furthermore, to look at the evolution of the amplitude of vibration during a welding stage, the ratio of these amplitudes is also studied, for example the amplitude of the anvil vibrations at the end of welding divided by the amplitude of the anvil vibrations at the beginning of stage 5. This is similar to the ratio presented in Figure 4-10. The ratios could therefore be related to the strengthening or weakening of the transfer of vibrations from the horn to the anvil. These features are listed in Table 5-7.

Table 5-7: Horn, anvil and ratio amplitude features

Envelope amplitude at the …	Anvil amplitude features	Horn amplitude features	Ratios of amplitudes features
Start of stage 2	A_2	H_2	$R_2 = A_2/H_2$
Start of stage 3	A_3	H_3	$R_3 = A_3/H_3$
Start of stage 4	A_4	H_4	$R_4 = A_4/H_4$
Start of stage 5	A_5	H_5	$R_5 = A_5/H_5$
End of welding	A_{end}	H_{end}	$R_{end} = A_{end}/H_{end}$

Table 5-8: Ratios of amplitudes calculated form the horn and anvil amplitudes

Relationship explored	Anvil	Horn
Change of amplitude in stage 2	$RA_{32} = A_3/A_2$	$RH_{32} = H_3/H_2$
Change of amplitude in stage 3	$RA_{43} = A_4/A_3$	$RH_{43} = H_4/H_3$
Change of amplitude in stage 4	$RA_{54} = A_5/A_4$	$RH_{54} = H_5/H_4$
Change of amplitude in stage 5	$RA_{End5} = A_{End}/A_5$	$RH_{End5} = H_{End}/H_5$
Change of amplitude from stage 3 to 5	$RA_{53} = A_5/A_3$	$RH_{53} = H_5/H_3$
Change of amplitude from stage 2 to the end of welding	$RA_{End2} = A_{End}/A_2$	$RH_{End5} = H_{End}/H_2$
Change of amplitude from stage 3 to the end of welding	$RA_{End3} = A_{End}/A_3$	$RH_{End3} = H_{End}/H_3$
Change of amplitude from stage 4 to the end of welding	$RA_{End4} = A_{End}/A_4$	$RH_{End4} = H_{End}/H_4$
Change of amplitude from stage 5 to the end of welding	$RA_{End5} = A_{End}/A_5$	$RH_{End5} = H_{End}/H_5$

While the amplitudes of the horn and anvil vibrations describe their amplitudes in absolute scale, it is possible that the changes in amplitudes which occur during a welding stage contain interesting information. For example, while one weld has a higher amplitude at the start of a stage than another weld, the second weld might have had a larger increase in amplitude during the previous stage, or it might show a larger increase across multiple stages. To explore this relation, the ratios of amplitude from one welding stage to another are calculated for both horn and anvil vibrations. The ratios are presented in Table 5-8.

5.2.2.3 *Time-and-amplitude-related features*

Time-and-amplitude-related features describe how the amplitude of the horn or anvil envelope changes during a welding stage or multiple welding stages. These features are useful to describe the rate at which the amplitudes change instead of the absolute amplitudes, since the horn and anvil vibrations showed different amplitudes. Similar to calculating a slope, they are calculated by dividing the change in amplitude in a welding stage by the duration of the welding stage, and are calculated for both horn and anvil envelopes. The features are listed in Table 5-9.

Table 5-9: Slopes of the amplitudes of the horn and anvil vibrations for each welding stage

Change in amplitude during…	Stage 2	Stage 3	Stage 4	Stage 5
Horn	$SH_2 = \frac{H_3 - H_2}{D_2}$	$SH_3 = \frac{H_4 - H_3}{D_3}$	$SH_5 = \frac{H_5 - H_4}{D_5}$	$SH_5 = \frac{H_{End} - H_5}{D_5}$
Anvil	$SA_2 = \frac{A_3 - A_2}{D_2}$	$SA_3 = \frac{A_4 - A_3}{D_3}$	$SA_5 = \frac{A_5 - A_4}{D_5}$	$SA_5 = \frac{A_{End} - A_5}{D_5}$

5.2.3 Steps of the statistical analysis

After having defined the features, they are now compared to the weld strength. A statistical analysis was done to evaluate the presence of a relationship between the features and the weld strength and train a multiple linear regression

algorithm. The analysis used correlation analyses, which investigate the presence of a linear relationship between the weld strength and individual features.

5.2.3.1 *Step 1: Correlation analysis between the features and the weld strength*

To assess the strength and direction of the linear relationship between individual features and the weld strength, a correlation analysis is performed. After checking the normality of the feature distributions using probability plots, it was found that some of the distributions were not Gaussian. For this reason, the correlation analysis was done using Spearman's rho ρ, returning the correlation coefficient and the corresponding p-value. Furthermore, the bootstrapped correlation coefficients and their confidence intervals were calculated for each feature[28]. All features which showed a significant correlation with the weld strength were kept for the next steps of the analysis, and the others were discarded. A correlation is taken to be significant when the p-value is smaller than 0.05 and the bootstrapped confidence interval is completely positive or completely negative, indicating with certainty that there is a positive or negative relationship with the weld strength.
Furthermore, the correlation coefficient is strong when its absolute value lies between 0.7 and 1, moderate when it lies between 0.4 and 0.7, and weak when it lies between 0.1 and 0.4. A negative sign indicates an inverse relation between the feature and the weld strength, and a positive sign indicates the opposite [28].

5.2.3.2 *Step 2: Feature selection*

Some features might exhibit strong correlations with each other, especially for features made from other features. Using all these features would lead to redundancy in the input given to the algorithm, which can lead to problems such as overfitting, longer computing time and difficulties interpreting the results. For this reason, a partial correlation analysis was done between the features which showed a correlation to the weld strength to isolate and better understand the specific association between the features being correlated while minimizing the impact of the other features. The partial correlation was again done using Spearman's rho and with bootstrapped confidence intervals. If features were found to be highly correlated with each other, then the one which was most strongly related to the weld strength was kept and the others discarded. For this purpose, highly correlated features were features for which the absolute value of at least

one of the limits of the corresponding bootstrapped confidence intervals was larger than 0.8.

5.2.3.3 *Step 3: Multiple linear regression*

The goal of these features is to estimate the weld strength within a single group made with the same welding parameters. According to Müller *et al.*, a common monitoring approach for USMW in the industry is a linear regression which uses welding time to estimate the weld strength [2]. This of course only works when welds are made using the total welding energy as a welding parameter given to the machine and not the total welding time. For this reason, single-variable linear regressions will be done to estimate whether the features derived offer an improvement compared to the current state of the art, and the reference will be a linear regression which uses the welding time to estimate the weld strength. Furthermore, multiple linear regressions will also be tested. As the goal of this study is only to investigate new features and not to investigate the impact of algorithms on the estimation, no further algorithms will be tested. For such studies, the reader is referred to the work of Müller *et al.* [2,7,36].

The linear regressions are of the forms:

Equation 2

$$y = m_1 x_1 + m_2 x_2 + \cdots + m_n x_f + b$$

where $x_1, x_2, \ldots, x_f$ are the f features used in the regression, $m_1, m_2, \ldots m_f$ are the corresponding coefficients, and b is the y-intercept. In the case of a single-variate regression, $f = 1$.

In a pre-study, single-variate linear regression, not shown here, were done, and an investigation of their residuals showed some outliers. To minimize the impact of the outliers, robust regressions were used for all regressions in this study [28]. The robust regressions were done using a bi-square weighting function with an initial tuning constant of 4.685, and the weights of individual measurements were iteratively reweighted, giving lower weight to points farther from model predictions in the previous iteration until the values of the weights converged to within a specific tolerance. Some of the residuals were also found to be non-normally distributed and with unequal variance, so bootstrapping was

used to get the bootstrapped confidence intervals at the 95% confidence level. The data was bootstrapped 3000 times, the mean of the regression coefficients were calculated as well as their standard errors. From the mean and standard errors the 95% confidence intervals were calculated.
To investigate how well a regression fit the data, the goodness of fit is described by the coefficient of determination R^2, which indicates the proportion of the variation in the outcome that can be predicted from the model. Since R^2 increases with the number of variables used in the regression, the adjusted R^2, calculated using Stein's formula, is used for the multiple linear regression [28]. To study the effect size, Cohen's f^2 is used, and is calculated using:

Equation 3

$$f^2 = \frac{R^2}{1 - R^2}$$

The interpretation of the effect size should be context specific. Since little context is available for the effect size of features to estimate weld strength in USMW, the conventional effect size interpretation will be used. The convention is that the effect size is small for values of f^2 smaller than a 0.15, medium for values smaller than 0.35, and large for values larger than 0.35 [37]. In the case of multiple linear regressions, the adjusted- R^2 is used to calculate f^2 instead of R^2.

In the multiple linear regressions, the features are introduced in two ways: first using a forced entry approach, in which all features are introduced at the same time, and then using a stepwise approach. In the stepwise approach used, combinations of features for which all features of the multiple linear regression are significantly related to the weld strength (p-value < 0.05) were sought. This stepwise approach starts with the single-variate regressions previously done, and a second variable from the remaining variables is added. If both variables are significantly related to the weld strength, then a third feature is added, and so forth until all features have been added or no new feature shows a significant relation to the weld strength.

5.2.4 Results and discussion

Table 5-10: Results of the correlation analysis between individual features and the weld strength. Rho is Spearman's correlation coefficient ρ, p is the p-value of the statistical test, and BCI is the bootstrapped confidence interval of the correlation coefficient.

Feature	Rho	p	BCI		Feature	Rho	p	BCI	
			Lower	Upper				Lower	Upper
T_5	0.401	0.010	0.084	0.646	RA_{End3}	0.330	0.038	0.005	0.591
D_3	0.342	0.031	0.019	0.603	RA_{End4}	0.366	0.020	0.045	0.650
D_5	-0.414	0.008	-0.661	-0.114	RA_{End5}	0.397	0.011	0.042	0.659
DD_{35}	0.501	0.001	0.214	0.702	RH_{43}	0.382	0.015	0.039	0.668
DL_{3345}	0.363	0.021	0.061	0.605	RH_{End4}	-0.436	0.005	-0.653	-0.171
DL_{5345}	-0.456	0.003	-0.679	-0.168	RH_{End5}	-0.526	<0.001	-0.737	-0.250
L_{34}	0.444	0.004	0.171	0.665	SA_2	-0.420	0.007	-0.665	-0.119
RA_{32}	-0.356	0.024	-0.653	-0.020					

The results for the features which showed a significant linear relation with the weld strength are shown in Table 5-10. The results for the complete list of features can be found in Appendix 10.5. Since, the correlation analysis explores and quantifies a possible linear relation between a feature and the weld strength, the results and discussions are based on the assumption of linear relations. Different results could be reached if non-linear relations are investigated.

Spearman's ρ, p-value and the bootstrapped confidence intervals for all features which showed a significant relation to the weld strength are shown in Table 5-10. The features showed either a weak or a moderate relation to the weld strength, with the strongest relation being showed by DD35 and RH_{End5}. The relation between these features, the weld strength and themselves can now be interpreted with respect to the welding process.

5.2.4.1 *Time-related features*

Looking at the time-related features, D_3 showed a weak positive relation to the weld strength. This would indicate that a longer time in stage 3 would lead to a stronger weld. This relation is even more significant because neither T_2 nor T_3 showed a significant linear relation to the weld strength. One possible explanation is that it would lead to a larger or denser weld, hence stronger. This interpretation is very simplistic, as in reality, the transition to stage 4 would happen once the weld reaches a strength larger than the force required to cause slipping at the horn and anvil interfaces. A longer stage 3 time would mean that the weld required a longer time to reach this threshold, keeping the horn-workpiece and workpiece-anvil interactions the same for different welds. A longer time to reach said threshold might mean the creation of a larger or denser but weaker weld than for a shorter stage 3. The weaker weld would then become stronger through stage 4 than the smaller or less dense weld. This theory is corroborated by the moderate positive relation between L_{34}, which includes the duration of both stages 3 and 4, and the weld strength, despite D_4 not showing a significant linear relation to the weld strength. The magnitude of the correlation coefficient of L_{34} was even larger than the one for D_3, showing a stronger relation to the weld strength. Furthermore, the partial correlation between L_{34} and D_3 shows a moderate positive correlation, ρ=0.49, p=0.011. This would indicate that the compound effect of a longer weld creation and strengthening does lead to a stronger weld, and that a longer strengthening stage alone does not. In addition, D_3 and DL_{3345} are strongly and positively correlated, ρ= 0.88, p<0.001, indicating redundancy between them.

T_5 and D_5 showed a moderate positive relation to the weld strength. The interpretations for T_5 and D_5 are similar: a later start time of stage 5 leads to a stronger weld, and a shorter time in stage 5 leads to a stronger weld. A possible explanation would be that longer times in stage 5 lead to more fatigue of the weld and a decrease in weld strength, which is corroborated by the explanation of Balz about how overwelding happens [1]. These two features show a strong negative correlation, ρ= - 0.76, p<0.001, which is expected since D_5 is created from T_5, and are therefore redundant.

Looking at the other features created from D_5 and D_3, almost all features showed a significant correlation to the weld strength. DD35 had a larger magnitude than D5 and D3, which could be due to the compound behavior of D3 and D5. The partial correlation analysis could not establish a linear relation between DD35 and D5, p=0.741, or DD35 and D3, p=0.484. DL5345 had a higher magnitude

than D5, probably due to it including D5 twice, and is also strongly and positively correlated to D5, $\rho = 0.78$, $p<0.001$. A linear correlation to T5 could not be established, $p=0.053$.
T_{end} did not show a significant linear relationship to the weld strength, with a p-value of 0.0605, despite being the reference case.

5.2.4.2 *Amplitude- and time-and-amplitude-related features*

Looking at the amplitude-related features, none of the horn or anvil amplitudes nor the ratios of anvil to horn amplitudes correlated significantly with the weld strength. The partial correlation coefficients and their respective p-values for the features that did correlate significantly to the weld strength are shown in Table 5-12 and Table 5-11.
RA_{32} and SA_2, which describe the change in amplitude during welding as a ratio or with regards to the welding time respectively, had a weak and moderate negative correlation to the weld strength respectively. This would indicate that the larger the change in the anvil amplitude through stage 2, the weaker the weld would be. This is an interesting result, as the anvil vibrations in stage 2 are either constant or slowly increasing. Possible explanations could be related to the anvil vibrations not increasing enough in stage 1 as much for the weaker welds than for the stronger welds and that being compensated in stage 2, or to a less slip between the workpieces for the weaker welds because of a less efficient shearing process, leading to a transfer of more energy to the anvil. The exact implications cannot only be guessed at this point, and further work would be needed to relate the change in amplitude during stage 2 to the welding process. Furthermore, they are strongly related to each other, $\rho=0.85$, $p<0.001$, as both depend on the change in amplitude during stage 2, indicating they are redundant.
The ratios of amplitudes at the end of stages 3, 4 and 5 to the amplitude at the end of welding are related to the welding process. RA_{End5} gives an indicator of the decrease in anvil amplitude during stage 5, while RA_{End4} and RA_{End3} give indications of all the changes which happened from stage 4 to the end of welding and stage 3 to the end of welding. RA_{End3}, RA_{End4} and RA_{End5} showed weak positive correlations to the weld strength, indicating that an increase in these ratios would correlate with an increase in weld strength. A linear relation between RA_{End4} and D_5 and RA_{End5} and D_5 cannot be established, their partial correlation to D_5 having p-values of 0.3 and 0.613 respectively, so the changes cannot be attributed to the duration of stage 5. Nevertheless, these features show

that the change in the amplitude of the anvil can be correlated to the weld strength. From
Table 5-12 and Table 5-11, RA_{End3} and RA_{End4} are strongly correlated, ρ=0.76 p<0.001, indicating some redundancy in using both of them to estimate the weld strength. Neither of them could be significantly correlated to RAEnd5, showing p-values larger than 0.05.

Table 5-11: p-values for the partial correlation of all amplitude-related features which correlated significantly with the weld strength

	RA_{32}	RA_{End3}	RA_{End4}	RA_{End5}	RH_{43}	RH_{End4}	RH_{End5}	SA_2
RA_{32}	0.000	0.113	0.454	0.269	0.811	0.059	0.855	0.000
RA_{End3}	0.113	0.000	0.000	0.611	0.311	0.292	0.640	0.006
RA_{End4}	0.454	0.000	0.000	0.075	0.147	0.827	0.499	0.200
RA_{End5}	0.269	0.611	0.075	0.000	0.152	0.118	0.040	0.120
RH_{43}	0.811	0.311	0.147	0.152	0.000	0.555	0.942	0.293
RH_{End4}	0.059	0.292	0.827	0.118	0.555	0.000	0.006	0.085
RH_{End5}	0.855	0.640	0.499	0.040	0.942	0.006	0.000	0.744
SA_2	0.000	0.006	0.200	0.120	0.293	0.085	0.744	0.000

Table 5-12: Partial correlation coefficients of all amplitude-related features which correlated significantly with the weld strength

	RA_{32}	RA_{End3}	RA_{End4}	RA_{End5}	RH_{43}	RH_{End4}	RH_{End5}	SA_2
RA_{32}	1.00	-0.32	0.15	0.23	0.05	-0.38	-0.04	0.85
RA_{End3}	-0.32	1.00	0.76	0.10	-0.21	-0.21	-0.10	0.52
RA_{End4}	0.15	0.76	1.00	0.36	0.29	-0.05	0.14	-0.26

RA_{End5}	0.23	0.10	0.36	1.00	-0.29	0.31	-0.41	-0.31
RH_{43}	0.05	-0.21	0.29	-0.29	1.00	0.12	-0.02	-0.21
RH_{End4}	-0.38	-0.21	-0.05	0.31	0.12	1.00	0.53	0.34
RH_{End5}	-0.04	-0.10	0.14	-0.41	-0.02	0.53	1.00	0.07
SA_2	0.000	0.006	0.200	0.120	0.293	0.085	0.744	0.000

RHEnd4 and RHEnd5 show a moderate negative correlation to the weld strength, indicating that a larger change in amplitude from the beginning of stage 4 or the beginning of stage 5 to the end of welding might be an indicator of a weaker weld. The horn amplitude does not change much during stage 4, which could mean that these two features are somewhat redundant, and the partial correlation between them returns ρ=0.53, p=0.006. No partial correlation could be established between them and the duration of stage 5 either, as the corresponding p-values were 0.197 and 0.235 respectively, so their dependence on D_5 cannot be studied. No linear correlation could be established between RH_{End4} and RA_{End4}, its counterpart in the anvil vibrations, as the p-value was larger than 0.8. A moderate negative correlation could be found between RH_{End5} and RA_{End5}, ρ=0.53, p=0.04. From knowledge of the welding process, it can be expected that the amplitude of the horn and anvil vibrations are related, indicating some redundancy between these two features.

RH_{43}, the ratio of horn amplitude from the beginning to the end of stage 3, has a weak positive correlation to the weld strength, indicating that horn vibrations which increase during stage 3 more than others might lead to stronger welds. This feature only correlates strongly with L_{34}, the duration of stages 3 and 4 combined, ρ= 0.54 p= 0.005.

5.2.4.3 *Feature selection*

Based on the partial correlation analysis and using knowledge of the welding process, some features can be selected to avoid redundancies in the feature set, which can otherwise lead to longer computational times, overfitting, and loss of interpretability of the contributions of individual features to an algorithm. For

this reason, DL3345, DL5345 and T5 can be discarded for D3 and D5 which are simpler, RA32 can be discarded for SA2 which correlates better to the weld strength. RAEnd3 is discarded for RAend4, as they are highly correlated and RAend4 correlates slightly better to the weld strength. RHEnd4, RHEnd5, L34 and RH43, RAend5 are kept as they do not correlate highly with any other feature. The final list of features kept is shown in Table 5-13.

Table 5-13: List of features kept after feature selection

D_3	D_5	L_{34}	RA_{End4}	RA_{End5}	RH_{End4}	RH_{End5}	SA_2	RH_{43}

5.2.4.4 *Single and multiple linear regressions*

Reference regression:

The results of the linear regression relating welding time and weld strength are shown in Figure 5-7 and
Table 5-14. The p-value, positive *m* and same-sign positive boundary confidence intervals (BCI) show that the relation between welding time and weld strength is significant, and that a longer welding time relates to a stronger weld. From Cohen's f-squared, the effect size is moderate, and R^2 shows that welding time accounts for only 13% of the variance in weld strength.

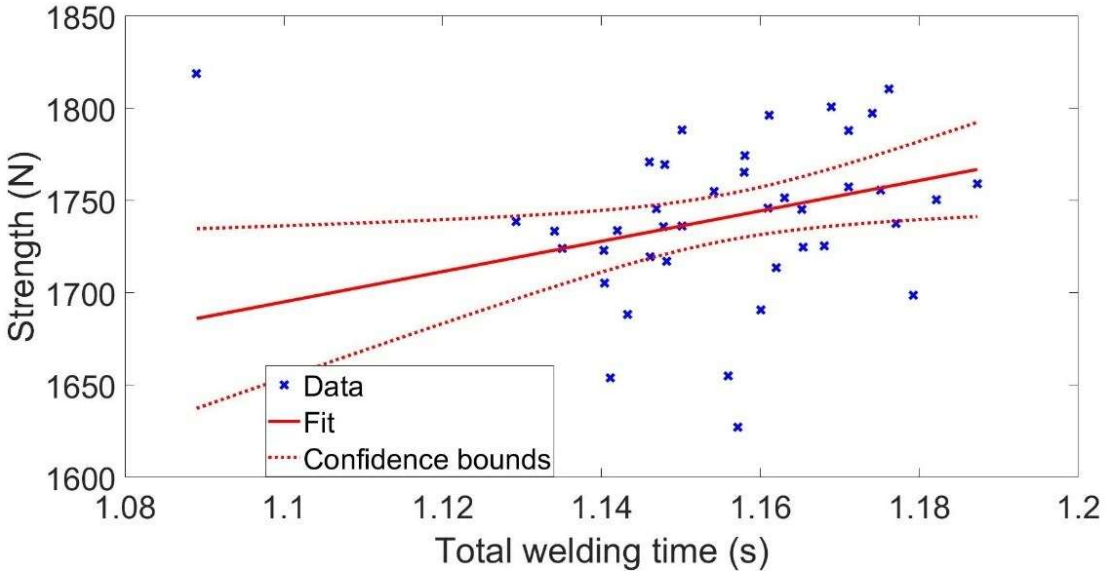


Figure 5-7: Robust linear regression relating the total welding time and the weld strength

Table 5-14: Results of the linear regression with welding time as an input. b and m are the y-intercept and slope shown in Equation 2, BCI is the bootstrapped confidence interval, R^2 is the coefficient of determination, f^2 is Cohen's effect size and RMSE is the root mean squared error.

p-value	b	m	BCI		R^2	f^2	RMSE
0.023551	790.58	822.36	42.91	1582.90	0.13	0.15	39.11

Single-variate regression:

Table 5-15: Result of robust linear regression of individual features to estimate the weld strength. p is the p-value, b and m are the y-intercept and slope shown in Equation 2, BCI is the bootstrapped confidence interval of the slope, R^2 is the coefficient of determination, F2 is Cohen's effect size and RMSE is the root mean squared error.

Feature	p	b	m	BCI		R^2	f^2	RMSE
D_3	0.038	1698.7	203.1	18.1	393.1	0.11	0.12	38.8
D_5	0.010	1812.3	-263.1	-449.7	-79.0	0.16	0.20	38.7
L_{34}	0.013	1647.1	177.8	50.7	301.8	0.15	0.18	39.3
RA_{End4}	0.004	657.1	1071.1	431.8	1709.1	0.20	0.25	38.9
RA_{End5}	0.005	-166.1	1979.8	765.4	3222.6	0.20	0.25	38.5
RH_{43}	0.014	117.8	1599.2	435.8	2751.0	0.15	0.18	39.6
RH_{End4}	0.022	3812.3	-2005.9	-3714.8	-315.0	0.14	0.16	38.8
RH_{End5}	0.001	5847.7	-4017.5	-5952.3	-2062.7	0.27	0.36	37.8
SA_2	0.007	1762.57	-10^8	$-16.6 * 10^7$	$-36.9 * 10^6$	0.17	0.21	39.9

The results of the single-variable linear regressions with the features selected in this thesis are shown in Figure 5-8, and the resulting p-values, equation coefficients, bootstrapped confidence intervals, R^2, and f^2 are shown in Table 5-15.

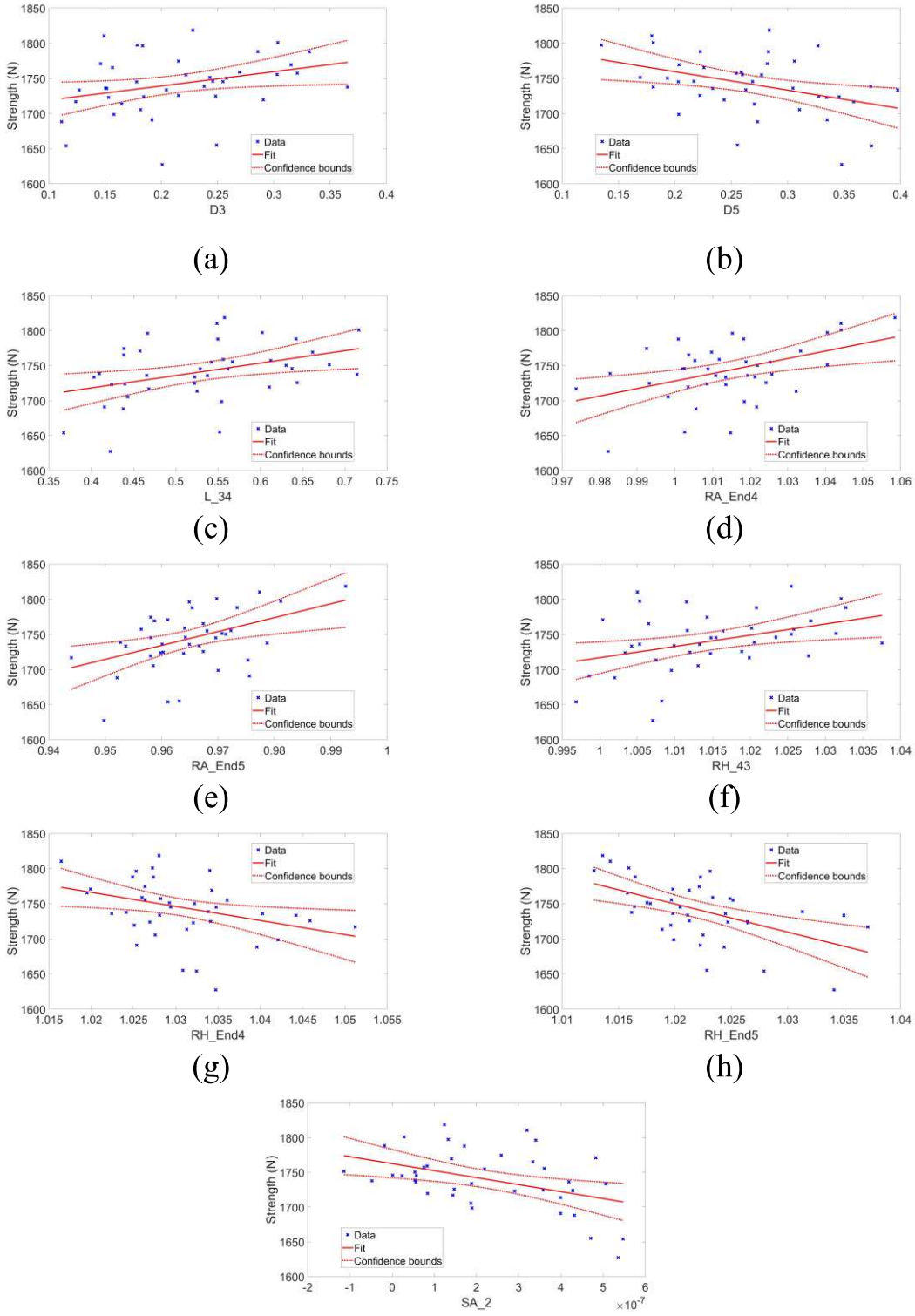


Figure 5-8: Linear regression of (a)D_3, (b)D_5, (c)L_{34}, (d)RA_{End4}, (e)RA_{End5}, (f)RH_{43}, (g)RH_{End4}, (h)RH_{End5} and (i) SA_2 vs weld strength.

The p-values and the same signs of the bootstrapped confidence intervals indicate that the relation between all features and the weld strength is significant. This is expected, since the features studied were found to be collinear with the strength.

The values of R^2 are moderate for RH_{End5}, RA_{End4} and RA_{End5}, indicating that these features explain a moderate amount of the variability in the strength. The other features showed lower R^2, ranging between 0.11 and 0.17. Cohen's f^2 shows a large effect size for RH_{End5}, suggesting that RH_{End5} is an important feature to estimate the weld strength. D_3 shows a small effect size, and the other features show a medium effect size. When compared to the regression using welding time, D_5, RA_{End4}, RA_{End5}, RH_{End5} and SA_2 show larger effect sizes, indicating improvements in the estimation. D_3, L_{34}, RH_{End4} and RH_{43} show comparable effect sizes than the welding time T_{end}, differing by up to 0.03, indicating that they would not necessarily improve the strength estimation done using the welding time.

If a single feature is used to estimate the weld strength, then either RA_{End5} or RA_{End4} should be used, despite showing a smaller correlation and effect size than RH_{End5}. This is because RH_{End5} needs a good identification of the start of stage 5. As discussed in Chapter 5.1, this cannot be done reliably using the horn vibrations, and monitoring the anvil vibrations would be required to use RH_{End5}.

Multiple linear regression:

The results of the forced entry regression are shown in Table 5-16. From the p-values, none of the features are statistically significant. This is confirmed by their bootstrapped confidence intervals including zero, except for RA_{End4} for which the interval is positive. However, the p-value of the overall model was 0.0158, indicating that the overall model is statistically significant. This means that while no single variable is significant on its own, the set of variables as a whole contributes significantly to explaining the variability in the weld strength. The R^2 and adjusted R^2 of the regression are 0.458 and 0.296, and Cohen's f^2 is 0.42. When compared to the regression using welding time, this multiple linear regression model explains 17% more of the variance in the weld strength and has a much larger effect size, indicating an improved fit. This forced entry regression also shows an improved performance compared to the single-variable regressions, having larger f^2 and adjusted R^2.

Table 5-16: Results of forced entry regression. m is the estimated slope for each feature, SE is the standard error for each estimate, p is the p-value of the statistical test, and BCI is the bootstrapped confidence interval of the slope estimates. For this forced linear regression, the corresponding b was 3470.2 N, with p=0.3882, SE=3963.2 N and BCI=[-2681.7, 9565.1].

Feature	m	SE	p	BCI	
D_3	81.44	235.58	0.73198	-288.158	451.9113
D_5	10.042	316	0.97486	-484.722	502.9828
L_{34}	-203.35	305.98	0.51138	-682.519	282.198
RA_{End4}	1264.8	772.94	0.11222	91.07108	2449.826
RA_{End5}	-889	1486.2	0.55421	-3193.59	1402.513
RH_{43}	937.47	1826.7	0.61157	-1967.68	3803.965
RH_{End4}	-763.53	1646	0.6461	-3349.41	1733.061
RH_{End5}	-2162	3471.9	0.53819	-7405.45	3263.79
SA_2	-9.57E+07	7.97E+07	0.23878	-2.2E+08	26879090

The p-value, R^2 and adjusted R^2 for the sequential multiple linear regressions are shown in Table 5-17. The coefficient estimates of each feature and their bootstrapped confidence intervals are shown in Appendix 10.6. From Table 5-17, only two-variable regressions and one three-variable regression were found. This is because adding another feature to the multiple linear regression would lead to one of the features or the y-intercept to be non-significantly related to the weld strength. All multiple linear regressions show a very significant estimate of the weld strength compared to using the mean, as shown by the very small p-values. Cohen's f^2 shows large effect sizes for all regressions which involve SA2, and medium effect sizes for the other regressions. This might indicate that the change in amplitude of the anvil vibrations in stage 2 has a strong

impact on the weld strength. Furthermore, the signs of the coefficients of the features used, shown in Appendix 10.6, are the same as the ones found for the single-variate regression in Table 5-15.

Table 5-17: Results of sequential multiple linear regression with all features showing a significant relation to the weld strength

Features			p	R^2	adjusted R^2	f^2
1	2	3				
D_5	RH_{End4}		0.00438	0.25	0.19	0.24
L_{34}	RH_{End4}		0.00284	0.27	0.21	0.27
RA_{End4}	D_3		0.00202	0.29	0.23	0.29
RA_{End4}	SA_2		0.000354	0.35	0.30	0.42
RH_{End4}	RH_{43}		0.00185	0.29	0.23	0.30
RH_{End4}	SA_2		0.000951	0.31	0.26	0.35
RH_{End4}	SA_2	RA_{End4}	0.00011	0.44	0.36	0.56

All sequential models show an improved fit compared to the welding time regression, showing larger effect sizes and adjusted R^2. The largest effect size and adjusted R^2 are found for the regression using RH_{End4}, SA_2 and RA_{End4}. This model explains more of the variance in weld strength and has improves the fit of all models tested so far, including the reference model, the forced entry model, and the single-variate models. All other sequential models show a worse or equal fit to the forced entry model.

5.2.5 Comparison to results from other studies

It is difficult to find results in other studies to which the features in this thesis can be compared. One source of difficulty is that studies in the literature often change the welding pressure, vibration amplitude, welding energy or time to create welds of different strengths [8]. This creates welds at different welding stages which are evaluated together, while this thesis presents features to estimate the weld strength within the same welding stage. These two types of studies can therefore not be compared. Another source of difficulty is when the welding parameters are kept constant, but workpiece variables are changed, for example rolling direction, hardness of the workpiece, or the presence of contaminants, and the study studies these different situations together, which can affect the results of the regressions [2,7,36]. For example, in the work of Müller

et al., running the regression for all workpiece variables studied instead of a single workpiece condition increased the R^2 from 0.35 to 0.7, keeping the features and the algorithm used constant.
To the knowledge of the author, at the moment of writing, only a single study describes the performance of a regression algorithm for a single set of workpiece conditions and the same welding parameters. In [2], Müller *et al.* discussed the use of features extracted from the weld depth and welding time to estimate the weld strength. In that study, they report R^2 values when running regressions for a single welding situation, in which a single set of welding parameters and workpiece parameters are used to create welds. This scenario is the same as the one used in this thesis in Group 3, in which the workpieces and welding parameters are the same. They report an R^2 value of 0.35 for a multiple linear regression using weld depth and welding time as inputs. This is a similar value to the R^2 value of the best-performing two-variable regression presented in this thesis. The best performing sequential model presented in this thesis, the three-variable sequential regression, performs therefore better than the regression presented by Müller *et al.*, since its adjusted R^2 is larger than the one of the two-variable regression. Based on this comparison, the
the features derived in this thesis seem to be at least as effective as the ones presented in [2], if not better. A more exact estimate is not possible without more detailed results from [2]. There is still a difference between the data set of Müller *et al.* and the one used in this thesis: when running a linear regression using the welding time as an input, similar to reference model used in this thesis, they report R^2 values between 0.52 and 0.66, and their figures show a clear collinearity between the welding time and weld strength. Meanwhile, the corresponding R^2 in this thesis was 0.13, and the scatter plot in Figure 5-7 shows a less pronounced collinearity. The impact of this difference on the performance of the features is unknown.

5.2.6 Conclusion on features for weld strength estimation

From this analysis, the best performing combination of features to estimate the weld strength would be a combination of features RH_{End4}, SA_2 and RA_{End4}. This would require to monitor both the horn and anvil vibrations and identify their amplitudes at the start of stage 4, the anvil amplitude at the start of stage 2 and its start time, and both the horn and anvil amplitudes and the time at the end of welding. If either the horn or the anvil have to be monitored and not both, then the combination of features RAEnd4 and SA2 can be used, showing the second-

largest effect size and coefficient of determination, as it only uses features derived from the anvil vibrations. Further work is required to compare the usefulness of these features to features presented in the literature, especially taking into account the use of different estimation algorithms.

5.3 Conclusion

In this chapter, features for real-time monitoring of the welding process and estimation of the weld strength were presented.

It was shown that the welding process can be monitored using the rate of change of both the horn and anvil envelopes at the welding frequency. Using the anvil vibrations and the rate of change of their envelopes, it is possible to monitor USMW throughout the five stages of welding, while only some stages can be identified from the horn vibrations. To identify the start of stage 5, the rates of change of both the anvil and the horn can be used, with the anvil-based monitoring being more effective than the horn's, as the start of stage 5 can be clearly identified in the anvil vibrations. Using the anvil vibrations, a stage 5 weld can be detected by a decrease in their amplitude, which can be detected by a change of sign of their rate of change after the stage 4 peak has occurred. Using the horn vibrations, a stage 5 weld can be identified by an increase of its amplitude compared to its stage 4 amplitude, which can be detected by a minimum in the rate of change of the horn envelope. With regards to real-time monitoring, the run time to calculate the rate of change and identify the start of stage 5 was found to take about 30 ms. This run time in addition to the run time required to produce the smoothed envelopes leads to a total run time of about 65 ms. This is short enough for a real-time monitoring of the welding process studied in this thesis, but shorter than the 50 ms requirement set in Chapter 0. A real-time implementation of the data processing approach suitable for all USMW processes could therefore not be established. Nevertheless, an optimized implementation of the data processing in a lower-level programming language or a relaxation of the 50 ms requirement, which was arbitrarily set, can still lead to a real-time monitoring implementation.

With regards to the strength estimation, features related to the welding process were extracted from the anvil and horn envelopes. These features described the time and amplitude dimensions of the vibrations. The linear relation of these features to the weld strength was quantified using a correlation analysis, and

those which showed a significant correlation were kept. A subset of these features was selected, using their partial correlations to avoid redundancies. These selected features were then used to run single-variate and multiple robust linear regressions to estimate the weld strength. Compared to only using the welding time as a feature, all selected features showed an improvement in the weld strength estimation. The best performing multiple linear regression model was a three-variate regression model which used the ratios of the horn and anvil vibrations from the beginning of stage 4 to the end of welding and the rate of change of the anvil vibration over all of stage 2 as inputs. This model had an R^2 of 0.36 and f^2 of 0.56, and requires the monitoring of both horn and anvil vibrations. If the vibrations of only one of them can be measured during welding, then a linear regression using RA_{End4} and SA_2 can be used, with $R^2 = 0.3$ and $f^2=0.4$, and if a single variable regression is to be done, then RA_{End4} or RA_{End5}, $R^2=0.2$, $f^2=0.25$ could be used. All three of these models show an improvement compared to using the welding time, $R^2=0.13$, $f^2=0.15$. For the strength estimation features, no real-time implementation was investigated as the run time would largely depend on the algorithm used to estimate the weld strength, and which was not investigated in this thesis.